Chin. Geogra. Sci. 2019 Vol. 29 No. 5 pp. 741–755
https://doi.org/10.1007/s11769-019-1069-4

Springer Science Press
www.springerlink.com/content/1002-0063

# Remote Detection of Varying Water Storage in Relation to Surfacial Temperature of Aral Sea

MU Guangyi[1], CHEN Li[2], HU Liangjun[1], SONG Kaishan[3]

(1. *Key Laboratory for Vegetation Ecology Science*, *Ministry of Education*, *Northeast Normal University*, *Changchun* 130024, *China*; 2. *Jilin Provincial Museum of Nature*, *Northeast Normal University*, *Changchun* 130117, *China*; 3. *Northeast Institute of Geography and Agroecology*, *Chinese Academy of Sciences*, *Changchun* 130102, *China*)

**Abstract:** Lake monitoring by remote sensing is of significant importance to understanding the lake and ambient ecological and environmental processes. In particular, whether lake water storage variation could predict lake surfacial temperature or vice versa has long fascinated the research community, in that it would greatly benefit the monitoring missions and scientific interpretation of the lake change processes. This study attempted to remotely detect the dynamics of the Aral Sea and pursue the relationships between varying lake water storage attributes and surface water temperature by using MODIS LST (Moderate-resolution Imaging Spectroradiometer Land Surface Temperature) 8-day composite products, satellite altimeter data, and actual meteorological measurements. Their associations with lake Surface Water Temperatures (SWT) were then analyzed. Results showed the lake water surface areas and elevations of the North Aral Sea tended to increasing trend from 2001 (2793.0 km$^2$, 13.6 m) to 2015 (6997.8 km$^2$, 15.9 m), while those of the South Aral Sea showed a decreasing trend during 2001 (20 434.6 km$^2$, 3.9 m) and 2015 (3256.1 km$^2$, 0.9 m). In addition, the annual daytime and nighttime lake SWT both decreased in the North Aral Sea, while only the daytime SWT in the South Aral Sea exhibited an increase, indicating a rising deviation of diurnal temperatures in the South Aral Sea during the past 15 yr. Moreover, a lower correlation was found between variations in the daytime SWT and storage capacity in the South Aral Sea ($R^2 = 0.33$; $P < 0.05$), no fair correlations were tested between lake water storage and daytime SWT in the North Aral Sea nor between lake water storage and nighttime SWT in either part of the sea. These results implied that climate change, if any at least during the research period, has no significant effects on lake dynamics over the two sectors of the Aral Sea with anthropogenic disturbances. However, climate change and human activities may overlap to explain complex consequences in the lake storage variations. Our results may provide a reference for monitoring the spatio-temporal variations of lakes, increasing understanding of the lake water storage changes in relation to the lake SWT, which may benefit the ecological management of the Aral Sea region, in the effort to face the likely threats from climate change and human activities to the region.

**Keywords:** Surface Water Temperature (SWT); lake water surface dynamics; lake water storage; Moderate-resolution Imaging Spectroradiometer (MODIS); the Aral Sea

**Citation:** MU Guangyi, CHEN Li, HU Liangjun, SONG Kaishan, 2019. Remote Detection of Varying Water Storage in Relation to Surfacial Temperature of Aral Sea. *Chinese Geographical Science*, 29(5): 741–755. https://doi.org/10.1007/s11769-019-1069-4

## 1 Introduction

Terrestrial water storage (TWS), representing the total loading capacity of all water bodies (lakes, rivers, reservoirs, wetlands, soil, and groundwater) above and beneath the earth's surface, plays a key role in regulating

Received date: 2019-01-24; accepted date: 2019-05-20
Foundation item: Under the auspices of State Special Funds for Research Infrastructure of China (No. 2015FY110500), National Natural Science Foundation of China (No. 41730104)
Corresponding author: HU Liangjun. E-mail: hulj068@nenu.edu.cn; SONG Kaishan. E-mail: songkaishan@neigae.ac.cn

global and regional water cycling, climate change, and water resource management (Zhang et al., 2011). TWS could interact with the atmosphere and oceans in the form of vertical and horizontal water or vapor fluxes, e.g., precipitation, evapotranspiration, and land surface/underground runoff discharge. Lake storage serves as an indicator, revealing the lake water balance, linked with lake inflows (e.g., precipitation and external runoff recharge) and outflows (e.g., evaporation and runoff discharge) (Chen et al., 2017). In addition, it provides moisture to the atmosphere, modulates heat dynamics of lake waters, irrigates farmlands, feeds household and industrial water consumption, and drives hydropower generation. Recently, Wang et al. (2018) confirmed the prevalent TWS decline over the entire exorheic region (–58.44 ± 27.75 Gt/yr, excluding Greenland and Antarctica). Lake water storage has been understood to be an essential component of TWS.

However, under current global warming scenarios, serious drought events have frequently occurred, and the storage of many lakes on earth have been shrinking, resulting in altered regional water cycles and even jeopardizing the utilization of global lakes, especially in the arid and semi-arid regions (Crosman et al., 2009; Bai et al., 2011). For instance, less storage often means reduced evaporation and warmer lake water. On the other hand, rising air temperature will heat lake water (especially the surface water) and increase lake surface evaporation, causing higher surface water temperature (SWT) and lower water storage (Song et al., 2016). Here, the SWT, similar to the land surface temperature (LST), is a key index representing the physical or even ecological conditions of a lake. Generally, variations in SWT can result in alterations in near-surface air turbulence, surface water evaporation, phytoplankton evapotranspiration, precipitation, and aquatic biomes of a lake and the land nearby; thus, SWT variations may affect the ecology, environment, and socio-economic development at the localities. Particularly, owing to the higher heat capacity of water, annual variations of SWT may depict long-term trends of climate and hydrological processes of a region (Crosman et al., 2009). In 2015, the American Geographical Union reported that SWT has been increasing at a rate of about 0.34℃ per decade in 235 lakes across the globe during 1985–2009, much higher than that in the oceans. Therefore, both SWT and the dynamics of lake water storage have been commonly considered to develop a viable proxy to examine lake ecosystems, lake hydrology, and global change issues (Gong, 2012; Luyssaert et al., 2014).

Although SWT and lake storage data are available for some lakes, in-situ measurements have been often limited because of the inaccessibility of faraway lakes and inaccuracies in sampling. Naturally, remote sensing has provided great opportunity for monitoring and assessing the climate and environmental change of an area (Wang et al., 2009; Hu et al., 2010; Wang et al., 2012; Shi et al., 2015; Song et al., 2016; Shi et al., 2019). To date, previous studies have been mainly focused on monitoring lake areas, water levels, and lake storage variations (Cretaux et al., 2011), as well as estimating lake SWT (Ke et al., 2014). Nonetheless, these studied lakes largely reside in the Tibetan Plateau (Zhang et al., 2011), Austria (Livingstone et al., 2001), and subarctic Alaska (Riordan et al., 2006), where anthropogenic impacts are typically weak. Because a lake surface is homogenous, spatiotemporal variations in the moderate-resolution imaging spectroradiometer land surface temperature (MODIS LST) are more stable in monitoring the thermal characteristics of lakes than those of land. Theoretically, estimation of lake storage is the integration of the difference between water level and bathymetry. As lake surface area is significantly correlated with lake water storage, satellite radar altimetry could be complementary to determining the effect on lake areas and surface elevation through short- and long-term dynamical processes. As lake surface area is often highly correlated with lake storage, using remote sensing to monitor lake water storage may be achieved by combining the extracted lake water surface area and elevation (Cretaux et al., 2011; Wang et al., 2013; Zhang et al., 2014), which will decrease the effect of the lakebed morphology. Thus, maintaining the integrity of the imagery in terms of error analysis and uncertainty reduction is essential. Thanks to the Geoscience Laser Altimeter System (GLAS) on board the Ice, Cloud, and Land Elevation Satellite (ICESat), lake elevation can be measured with higher vertical precision (about 10 cm) (Zhang et al., 2011). In short, the MODIS LST data products, MODIS reflectance products, and ICESat/GLAS data are ready for use in monitoring and evaluating lake dynamics at certain spatiotemporal scales.

Wang et al. (2018) reported that approximately two-thirds of the global endorheic water loss (–73.64 ±

7.74 Gt/yr) may arise from central Eurasia, where 10% of the entire zonal loss was concentrated on the Aral Sea Basin (including nearby watersheds receiving transbasin diversion). Because of the predominantly periodical desiccating climate and intensive anthropogenic impacts, the Aral Sea storage varied significantly, exhibiting substantial shrinking since the 1960s. Consequently, the ecology and environment of the Aral Sea region has aroused wide public concern. However, previous studies were more focused on water levels and sedimentation of the Aral Sea (Micklin, 2010), anthropogenic activity (Boomer et al., 2009), and hydrologic responses to climate change and irrigation in the region, while lacking data pertaining to quantified temperature variations in relation to lake dynamics. Throughout much of history, the Aral Sea, together with its feeding rivers, served as a cultural and economic provider for the region, which made understanding the mere effects of lake dynamics and lake surface temperature variations a complicated challenge. Thus, long-term monitoring of lake dynamics, including lake area, elevation, and storage capacity in relation to SWT of the Aral Sea, might be of much help in better understanding and managing the Aral Sea ecology and environment.

Based on the above, this study aimed to: 1) analyze the long-term variations in lake area, lake elevation, lake storage, and daytime and nighttime SWTs of the Aral Sea by using multi-source remote sensing data; and 2) elucidate the likely associations between lake parameters and SWTs of the Aral Sea. Results from this research may help disentangle the localized environmental and ecological processes, and provide scientific supports for regional water resources and ecosystem management in similar lake-oriented arid and semiarid regions.

## 2 Materials and Methods

### 2.1 Study area

The Aral Sea (43°24′N–46°56′N, 58°12′E–61°59′E), lying on the border of Kazakhstan and Uzbekistan, was once the world's fourth largest lake (Fig. 1). It is located in the arid continental monsoon climate zone, with a mean annual temperature of 9.4℃, and an average annual precipitation ranging from 100 to 440 mm. The Aral Sea is a terminal and enclosed lake, fed by certain inland rivers such as the Amu Darya River and the Syr Darya River. Precipitation and groundwater are the major hydrological factors controlling the lake water storage. Before the 1960s, the Aral Sea area ($6.8 \times 10^4$ km$^2$) varied mildly and remained fairly stable, with a lake water level of approximately 53 m. Since the 1960s, the Aral Sea began shrinking because of the local need for agricultural irrigation. As a result, the Aral Sea was separated into two parts—the North Aral Sea and the South Aral Sea. In 2008, the North Aral Sea was approximately 3300 km$^2$ in area, and the South Aral Sea was about 8200 km$^2$.

### 2.2 Data sources and preprocessing

(1) MODIS products. The National Aeronautics and Space Administration (NASA) provides MODIS products for free at http://ladsweb.nascom.nasa.gov/data/

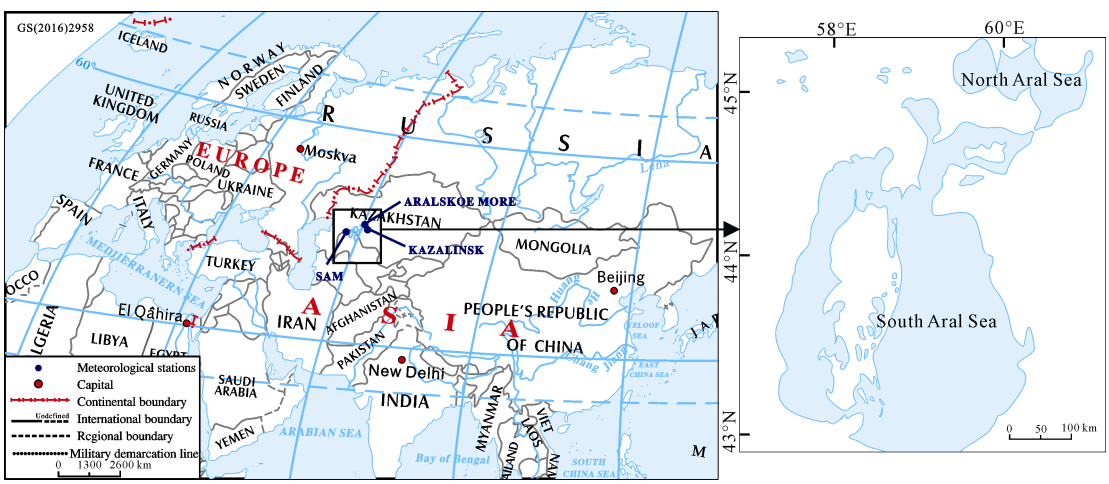


**Fig. 1** Location of the Aral Sea. The left map were from Ministry of Natural Resources of the People's Republic of China (http://bzdt.ch.mnr.gov.cn)

search.html, with the path number h22v04 for the Aral Sea. MODIS products used in this study included land surface temperature (MOD11A2) and surface reflectance products (MOD09A1). Particularly, consistent data sources can ensure good temporal matching between lake temperatures and area calculations. MOD11A2 can provide daytime and nighttime temperatures at a resolution of 1000 m in an 8-day gridded level 3 product, as was used to analyze lake SWTs in the Aral Sea. The acquired MOD11A2 8-day composite product contained 46 stacked layers, each including daytime and nighttime temperature records. After mosaicking through MRT (MODIS Reprojection Tool), the MODIS LST 8-day composite images were projected to Albers in GeoTIFF by using the nearest-neighborhood interpolation method. By contrast, MOD09A1 can provide Band 1 to Band 7 at a resolution of 500 m in an 8-day gridded level 2 product. The MODIS products temporally span 15 yr (from 2001 to 2015).

(2) ICESat/GLAS data. The ICESat, launched by NASA Earth Science Enterprise, is commonly used to measure ice sheet mass balance, cloud and aerosol heights, and land topography and vegetation cover. In this study, GLAS14 from ICESat was used to calculate the elevation of the Aral Sea with a temporal span of 7 yr (launching in 2003 and ending in 2009). In general, ICESat/GLAS provides two types of pulsed laser waves (1024 nm and 532 nm) with a spot diameter of approximately 70 nm and an operating frequency of 40/s. The ICESat/GLAS repeats once each eight days. More details about ICESat/GLAS can be found in Dessler et al. (2006).

(3) Meteorological data. The average air temperatures at the three meteorological stations (ARALSK, KAZALY, and SAM in Kazakhstan) in the Aral Sea area were used to validate the temperature data extracted from MOD11A2. Then, the air temperatures 2-m above the ground were obtained for free from the website http://www.ncdc.noaa.gov at the National Climate Data Center (affiliated with the National Oceanic and Atmospheric Administration-NOAA). Likewise, at each meteorological station, daily temperatures were averaged from ground records. To analyze the monthly (i.e., lake freezing and thawing months) and annual SWT dynamics of the region, daytime and nighttime temperatures during March to October were considered.

## 2.3 Lake area, elevation, and storage capacity extraction

### *2.3.1 Lake water surface area*

Generally, water strongly absorbs light in the near-infrared (NIR) band with lower reflectance, while the land surface has higher reflectance. For this sake, the Normalized Difference Water Index (NDWI) threshold method has been commonly used (Song et al., 2016). NDWI can well extract the lake water area information by analyzing the histogram of NDWI at land-water interfaces to determine an optimal threshold (Sun et al., 2012). Under fine conditions, a positive NDWI value indicates that the land is covered by water and ice, a zero value corresponds to rock and soils, and a negative value indicates vegetation. McFeeters et al. (1996) reported that choosing the green band could yield better performance for NDWI as:

$$NDWI = (G - NIR) / (G + NIR) \quad (1)$$

where $G$ and $NIR$ represent the reflectance in the green band (band 4, 545–565 nm) and $NIR$ band (band 2, 841–876 nm) for MODIS, respectively.

In this study, due to the significant area variations in the Aral Sea, we determined the thresholds through the NDWI histogram and human-computer interaction. First, each scene of the MODIS09A1 (in hierarchical data format, sinusoidal projection) product was re-projected to a more commonly used UTM projection (Universal Transverse Mercator, WGS84) with the nearest neighborhood re-sampling method in MRT: 1) NDWI results were created using Eq. (1) with 'Band Math' tool in ENVI 5.3 environment. 2) A rule was used to identify water bodies and non-water by the tool 'Decision Tree' with NDWI Gt 1.0 (temporary threshold). However, the NDWI thresholds of each image with the ratio-based index were sensitive to atmospheric variations at spatiotemporal scales. Thus, to obtain the optimal threshold for each image, the initial threshold (temporary) was determined from wave troughs of waters and non-waters in the histogram with bimodal distribution. Then, the initial threshold (temporary) was adjusted until a best match between waters and shores (MODIS, Red-Green-Blue 'true-color' images at a resolution 500 m) was obtained for different scenes by human-computer interaction. If the NDWI value of a pixel agreed well with the rule, the pixel would be classified as water. Consequently, the thresholds in the water

extraction ranged from 0.9 to 1.2 throughout the repeated comparisons.

#### *2.3.2 Lake elevation*

Lake water levels were retrieved from the ICESat/GLAS orbital measurements with three steps. First, latitude, longitude, reflectance, and atmospheric radiation from the ICESat/GLAS14 laser spot were evaluated through error correction, with the Global Positioning System (GPS) coordination points acquired from file *batch_read_altimetry.sav* in the IDL (Interface description language) procedure. Afterward, the GPS points were converted into vectors. Next, the lake water area boundary that was identified by MOD09A1 (see Section 2.3.1) with the ICESat overpass was used to obtain the orbital geographical location information. We chose the annually smallest area of the Aral Sea (extracted by MOD09A1, see Section 2.3.1) for the period March to October to build a buffer in terms of avoiding the influence of the boundary interface between water and land. In the meantime, all the lake boundaries were buffered by 1000 m to remove the laser spots outside the lake range. Then, all the lake elevation measurements of laser spots were extracted according to the smallest area. Next, each laser spot including the water surface level information from ICESat data was used to remove the influence of the geoidal surface. ICESat GLAS data itself were provided with a geo-potential model of the Earth as EGM96 (Earth Gravitational Model 1996). Hence, the water surface level information from each laser spot of the ICESat data was represented as the lake water level directly. As a result, the lake water level at a certain moment (e.g., April 2009) was the average value of all the valid laser spots within a least lake area (see Section 2.3.2) at the same moment.

According to a statistical analysis of lake water elevation during each observational day, some anomalous laser spots that exceeded the standard deviations of the lake water elevation 0.1 were deleted. As for the omitted years (before 2003 and after 2009), lake water level elevations were calculated through regression models between the area of the cutting laser spots during the period 2003–2009 and the corresponding elevations.

#### *2.3.3 Lake water storage capacity*

Lake water storage capacity refers to the largest volume defined by the present horizontal curved water surface and certain bed morphology. Generally, differences in the relative dynamic storage capacity $Q_C$ at a specific time point can be calculated by using the simultaneous area and water elevation of a lake. For instance, if $Q_{t1}$ indicates the storage capacity at time point $t_1$, and $Q_{t2}$ indicates the storage capacity at time point $t_2$, then the dynamic capacity $Q_C$ between $t_1$ and $t_2$ can be described as:

$$Q_C = Q_{t_2} - Q_{t_1} = \Delta Q + A + B \tag{2}$$

where $Q_{t1}$ is the storage capacity at moment $t_1$, $Q_{t2}$ is the storage capacity at the moment $t_2$; $A$ and $B$ represent terrain parameters. If the terrain is unknown, compared with the significant variations of lake storage (e.g., the Aral Sea), the variations of terrain parameters can be ignored, especially in long-time observations (i.e., 2001 to 2015).

Combining with the dynamic lake area from MODIS09A1 products and lake water level from ICESat data, the lake dynamic storage could be presented as:

$$Q_c = \sum_i^m P_{t_{1i}} \times E_{t_1} - \sum_i^n P_{t_{2i}} \times E_{t_2} \tag{3}$$

where $P_{t_1}$ is the area of the signal pixel at moment $t_1$, $m$ is the sum of lake pixels at moment $t_1$; $P_{t_2}$ is the area of the signal pixel at moment $t_2$, $n$ is the sum of lake pixels at moment $t_2$; $E_{t_1}$ is the water level at moment $t_1$ from ICESat data, and $E_{t_2}$ is the water level at moment $t_2$ from ICESat data.

### 2.4 Lake surface water temperature extraction and validation

As noted above, the pre-treated MOD11A2 was extracted in four layers, i.e., daytime LST (overpass time was at about 10:30 a.m. in the local time), nighttime LST (overpass time was at approximately 22:30 p.m. in the local time), and corresponding quality-control (QC) images (daytime and nighttime). In reference to the method proposed by Ke et al. (2014), we removed the suspicious pixels and deduced the valid ones from QC information and median filtering in the time-series LST data stacks resulting from the presence of cloud contamination. According to the LST data quality flag files stored in the QC file, all the pixels with LST errors less than 1000 (i.e., QC = 0, 1, 5, 17, 21) were kept, while the others were removed. However, pixel values could not represent the true LST; therefore, a conversion through band operation is often necessary to obtain the actual surface temperatures. The band operation formula

for LST images was used to transfer DN (Digital Number) to degrees centigrade as follows:

$$T = DN \times 0.02 - 273.15 \quad (4)$$

where $T$ is the surface temperature value (℃) and $DN$ is the gray value of an LST image.

A total of 704 pieces of images over the Aral Sea were acquired during 2001–2015. The data processing procedure is shown in Fig. 2. The mean lake SWT was derived from all the pixels in the daytime or nighttime LST images from March to October. However, dynamic lake areas often resulted in an inaccurate retrieval of temperatures between water and land. To avoid such errors, we selected a fixed common area—the minimum lake area in all the years as a range boundary of the used MODIS temperature images.

In addition, the air temperatures acquired from 2-m high above the ground over the three meteorological stations (ARALSK, KAZALY, and SAM in Kazakhstan) were applied to validate the lake daytime and nighttime temperatures extracted from MODIS LST. As shown in Fig. 3, MODIS LST was in fine agreement with monthly average temperatures of the meteorological stations, with $R^2 = 0.73$ (KAZALY), 0.69 (SAM), and 0.64 (ARALSK) ($P < 0.01$) in the North Aral Sea. Likewise, the South Aral Sea was found to have similar agreement, with $R^2 = 0.77$ (KAZALY), 0.73 (SAM), and 0.68 (ARALSK) ($P < 0.01$). In general, a consistently increasing temperature change over the Aral Sea was found in terms of air temperature and LST during the recent decades. By contrast, the lake MODIS LST better reflects the real surface temperature variations than land MODIS LST because of the homogeneous lake surface.

### 2.5 Statistical analysis

Regression and correlation analyses were conducted to examine the relationships between variables (temperatures from MODIS LST and meteorological stations, lake surface water area, lake water level, and lake water storage). Statistical differences between variables were assessed with analysis of variance (ANOVA) by defining three significance levels in which no significance is represented by $P > 0.05$, significant corresponds to $P < 0.05$, and highly significant corresponds to $P < 0.01$.

## 3 Results

### 3.1 Dynamics of lake area, elevation and storage capacity

#### *3.1.1 Lake surface water area*

Fig. 4 demonstrates the annual variations in the examined Aral Sea areas during 2001 to 2015. According to the area extraction by the NDWI method from MODIS09A1 (Section 2.3.1), the smallest South Aral Sea area was recorded in 2014 (3883.35 km$^2$), and the highest record area was recorded in 2001 (21 684.60 km$^2$). Despite a slight increase in 2010 (9246.80 km$^2$), the area decreased throughout 2010 to 2014. By contrast, an increase in the lake area was observed in the North Aral Sea during the past 15 yr (Fig. 4). In 2006, the North Aral Sea increased to 3293.1 km$^2$ in area and then remained at a stable level.

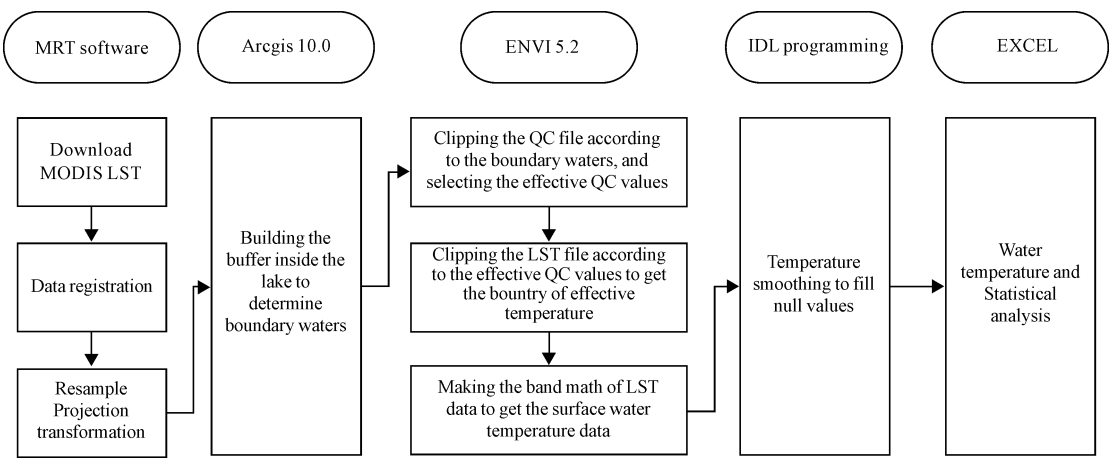


**Fig. 2** Processing flow scheme for MODIS LST data. MODIS LST is Moderate-resolution Imaging Spectroradiometer Land Surface Temperature; MRT is MODIS Reprojection Tool which could resample and make a reprojection transformation. Quality-control (QC) images (daytime and nighttime) of MODIS LST store LST data quality flag files and information. IDL (Interface description language) procedure of ENVI 5.2 is aimed to smooth the file null values.

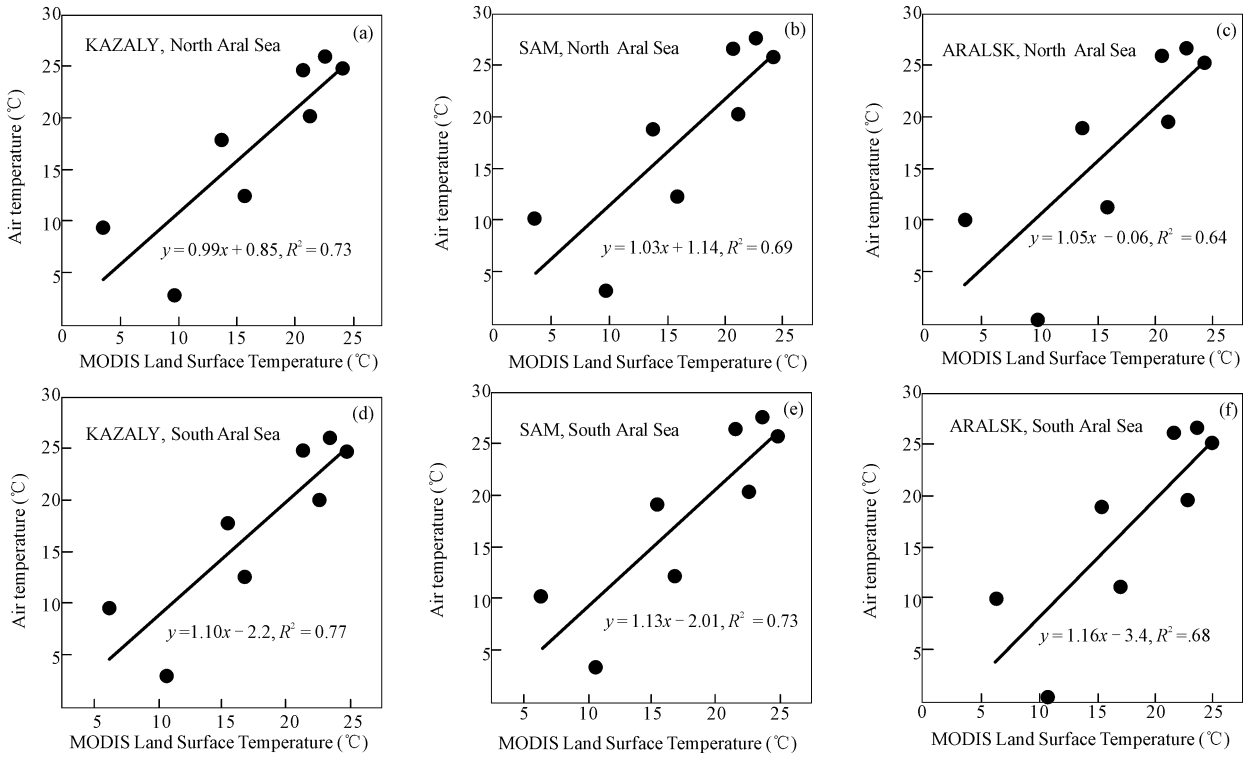


**Fig. 3** Regression analysis results of monthly averaged temperatures between MODIS LST (Land Surface Temperature) and meteorological stations ($N$ = 8, March to October) from 2001 to 2015: (a) ARALSK, (b) KAZALY and (c) SAM in the North Aral Sea; (d) ARALSK, (e) KAZALY and (f) SAM in the South Aral Sea. The monthly averaged air temperatures at the three meteorological stations (ARALSK, KAZALY and SAM) in the Aral Sea watershed were obtained for free from the National Climate Data Center (affiliated with NOAA). Also, the monthly averaged MODIS LST included daytime and nighttime values. To be consistent with the temporal variations (March to October) of the lake area and levels from MODIS09A1 and ICESat, the temperatures from both MODIS LST and meteorological stations were averaged from 2001 to 2015. Thus, the monthly averaged temperatures were acquired throughout March to October ($N$ = 8).

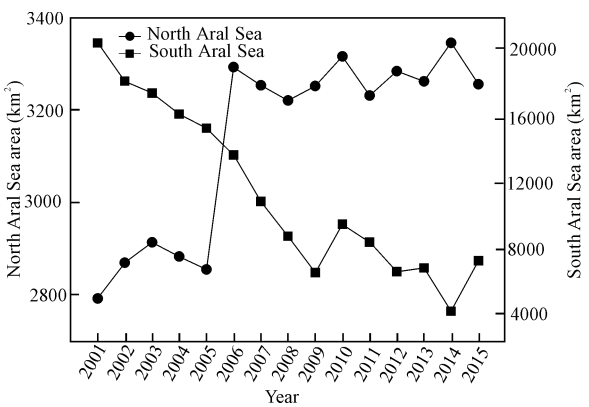


**Fig. 4** Yearly average area of the North and South Aral Seas from 2001 to 2015

### *3.1.2 Lake water elevation*

To supplement the omitted elevation data during the no-record years (because working time was from 2003 to 2009 for GLAS14), regressions between the lake water elevation and areas were constructed for the North and South Aral Seas (Fig. 5). A positive quadratic polynomial relationship between the lake area and elevation was found for the North Aral Sea ($R^2$ = 0.86; $P$ < 0.01), and a linear relationship between lake area and elevation was found for the South Aral Sea ($R^2$ = 0.87; $P$ < 0.01). In referring to the regression results, water elevation for the omitted years was calculated (Fig. 5c). As a result, the average water elevation of the South Aral Sea was 1.76 m during 2001–2015, showing a decreasing trend. Likewise, a stable tendency in lake water elevation was found in the North Aral Sea, revealing an average water elevation of 13.89 m. These results were in line with the areal variations of the Aral Sea.

### *3.1.3 Lake water storage capacity*

To some extent, lake water area and elevation could reflect the dynamics of an entire lake. The lake water storage calculated by water area and elevation is shown in Fig. 6. In general, the South Aral Sea exhibited higher storage capacity variations than the North Aral Sea. In

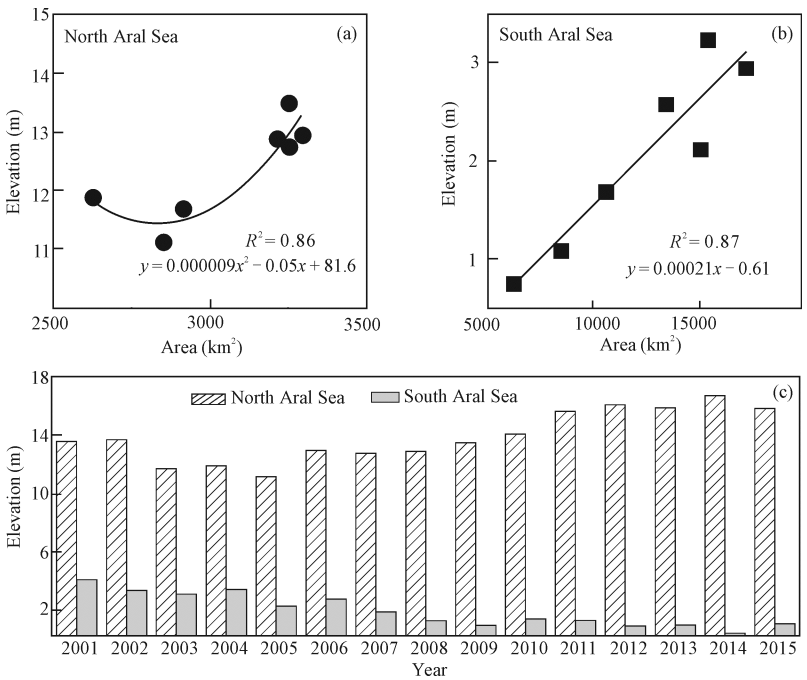


**Fig. 5** Elevation variations in the Aral Sea: (a) regression model between lake area and lake elevation at the North Aral Sea during 2003–2009; (b) regression model between lake area and lake elevation at the South Aral Sea during 2003–2009; (c) elevations of the Aral Sea during 2001–2015. Due to the water elevation was extracted from ICE/GLAS (2003–2009), thus the omitted years (e.g., 2001–2002 and 2010–2015) were calculated by the functions in Figs. 5a and 5b.

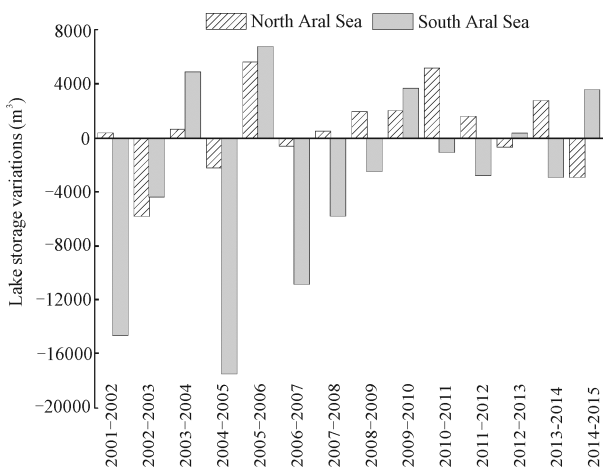


**Fig. 6** Variations of lake storage in the North and South Aral Seas (negative values representing a decrease in area over the past two years and positive values representing an increase over the same period). The variations were calculated by Eqs. (2)–(3). 2001–2002 represents the variations of lake storage from 2001 to 2002, and the remaining can be done in the same manner.

particular, the South Aral Sea exhibited huge fluctuations in lake water storage, revealing descending variations as the lake water area and elevation during 2001 to 2015. Specifically, higher lake storage variations in the South Aral Sea were observed in 2001–2002 (−14 575.5 m$^3$), 2004–2005 (−17 457.8 m$^3$), and 2006–2007 (−10 820.8 m$^3$). By contrast, lake storage variations in the North Aral Sea revealed milder fluctuations,,with critical variations observed in 2002–2003 (−5808.8 m$^3$), 2005–2006 (5563.4 m$^3$), and 2010–2011 (5139.7 m$^3$), respectively.

### 3.2 Temporal patterns in SWT

#### *3.2.1 Annual SWT dynamics*

SWTs of the Aral Sea ranged from 14.0℃ to 20.4℃ during 2001–2015 (Fig. 7). In general, in the North Aral Sea, daytime temperature and nighttime temperature both showed a consistent trend before 2012. Such results can also be found in the South Aral Sea before 2011. To this, Song et al. (2016) suggest that smaller diurnal temperature deviations often exist for a lake with smaller area and shallower depth. Clearly, our results agree well with this conclusion.

#### *3.2.2 Monthly SWT dynamics*

During 2001–2015, the monthly SWT increased at the beginning of each March, with the daytime temperature at approximately 11.5℃ in the North Aral Sea (Fig. 8a)

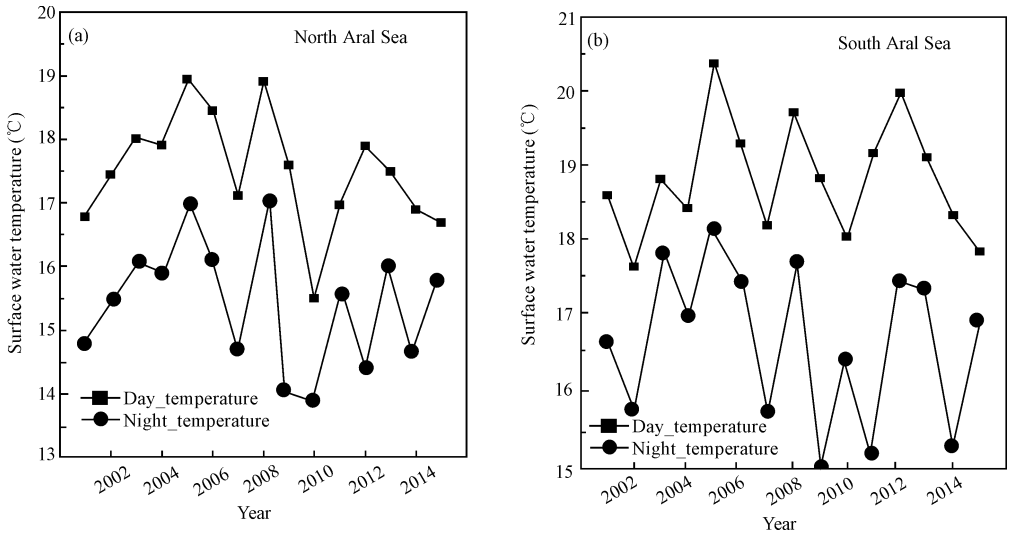


**Fig. 7** Average annual temperatures from MODIS LST during 2001–2015 in the North (a) and South (b) Aral Seas

and 12.4℃ in the South Aral Sea (Fig. 8b), and nighttime temperature at 10.2℃ in the North Aral Sea and 9.8℃ in the South Aral Sea. In April, the daytime and nighttime SWTs in the North Aral Sea were 6.6℃ and 6.2℃, respectively, while those in the South Aral Sea were 10.1℃ and 9.3℃. The highest SWTs emerged in June, i.e., 23.1℃ for daytime and 22.5℃ for nighttime in the North Aral Sea, and 22.1℃ for daytime and 21.6℃ for nighttime in the South Aral Sea. During this period, the lake SWT in the South Aral Sea exhibited higher daytime/nighttime values than in the North Aral Sea likely because of the effect of the lake depth. In addition, this warmer period corresponded to greater lake performance. At the end of each October, the daytime SWT fell to 4.1℃ in the North Aral Sea and 7.1℃ in the South Aral Sea, while the nighttime SWT decreased to 2.3℃ in the North Aral Sea and 5.2℃ in the South Aral Sea.

### 3.3 Correlations between SWT and lake dynamics

#### *3.3.1 Lake SWT vs. lake area*

Regression analysis between the variations in area and SWT in the South and North Aral Seas during 2001–2015 was conducted (Fig. 9). The results indicate that there were no fair correlations between daytime temperature variations ($R^2$ = 0.05) or nighttime temperature variations ($R^2$ = 0.02) and lake area variations for the North Aral Sea (Fig. 9a). By contrast, a weak correlation between daytime ($R^2$ = 0.11) or nighttime SWT variations ($R^2$ = 0.19) and lake area variations was found for the South Aral Sea (Fig. 9b).

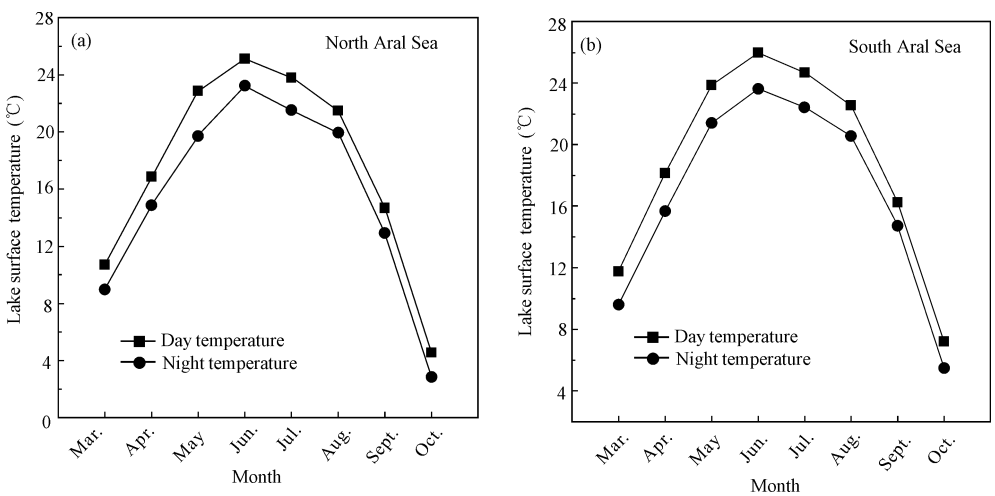


**Fig. 8** Monthly temperatures of MODIS LST during 2001–2015 in the (a) North and (b) South Aral Seas

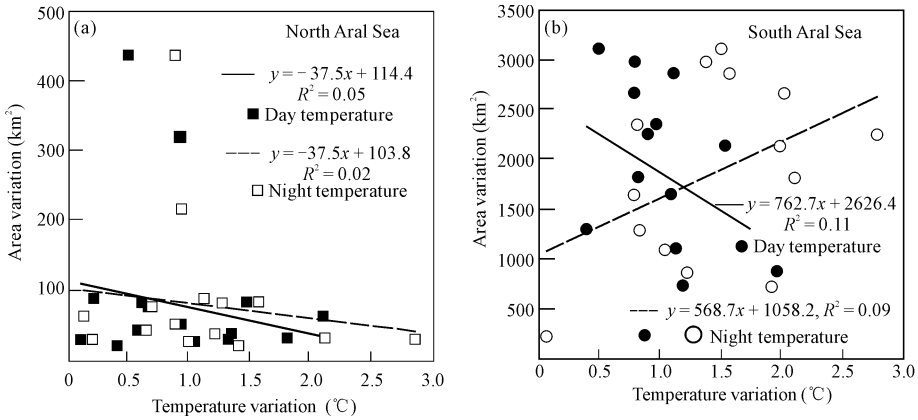


**Fig. 9** Correlations between lake surface water area variations and SWT variations in the (a) the North Aral Sea and (b) the South Aral Sea

### *3.3.2 Lake SWT vs. lake elevation*

Regression analysis linking SWT and lake elevational variations in the South and North Aral Seas throughout 2001 to 2015 are presented in Fig. 10. The results revealed that there was no positive correlation between lake elevation and SWT variations during the period in the North Aral Sea ($R^2$ = 0.02 for daytime and $R^2$ = 0.01 for nighttime, Fig.10a). By contrast, though there were also no positive correlations between lake SWT and lake elevational variations in the South Aral Sea, a weak correlation was found between the daytime SWT variation and the lake elevation variation in the South Aral Sea ($R^2$ = 0.22, Fig. 10a).

### *3.3.3 Lake SWT vs. lake storage capacity*

Fig. 11 revealed that there existed correlations between lake storage variation and daytime SWT variation in the South Aral Sea ($R^2$ = 0.33, $P$ < 0.01); the other three situations all indicated poorer correlations in the lakes. However, this could not be extrapolated to the North Aral Sea or nighttime conditions, which may be due to certain complicated influences, such as increasing anthropogenic activities around the lakes and variations in nighttime lake SWT, affected by unknown factors other than lake water storage.

## 4 Discussion

### 4.1 Human activities likely impacting the Aral Sea

Previous studies reported that over the past three decades, discharge of feeding rivers significantly varied in the Aral Sea region, crucially impacting the lake elevation (Cretaux, 2013). Since the 1950s, traditional nomadic herding was converted into cropping regimes in the region, owing to the decision of the former Soviet central planners that the Mid-Asian countries should be a cotton production center. To adapt to such a change, many irrigation and water diversion engineering projects were established in the Aral Sea region. Before the

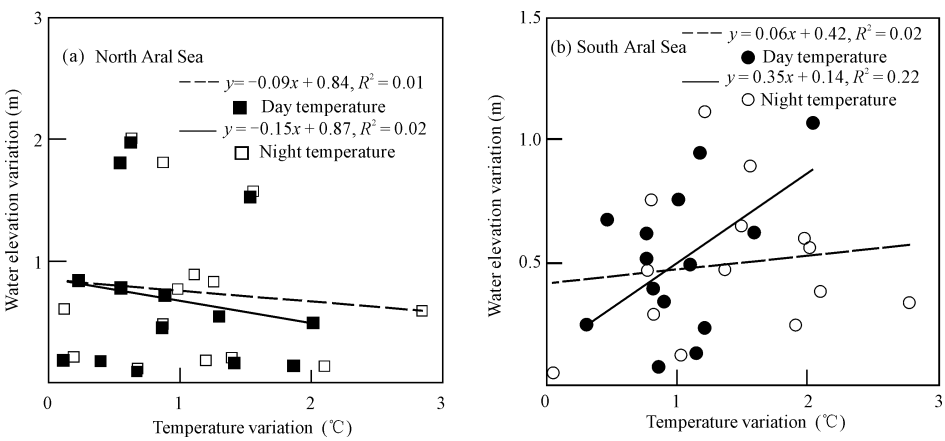


**Fig. 10** Correlations between lake water elevation variations and lake SWT variations in the Aral Sea. (a) the North Aral Sea; (b) the South Aral Sea.

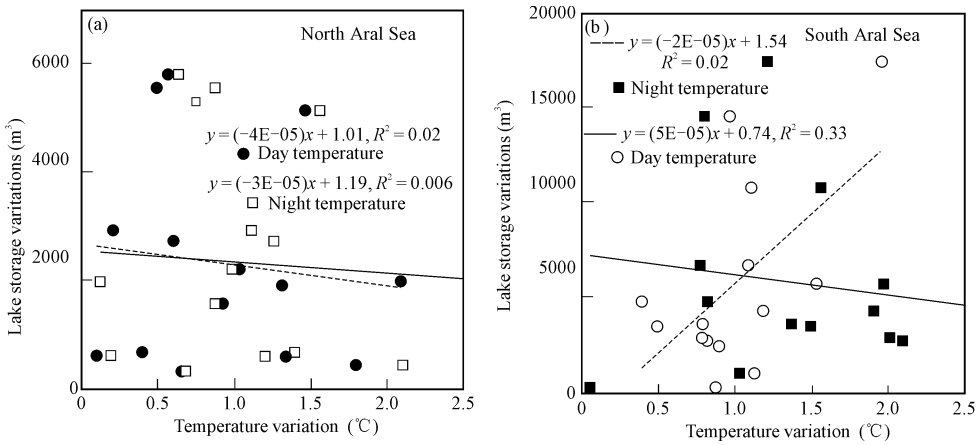


**Fig. 11** Correlation analysis between lake storage variations and SWT variations. (a) the North Aral Sea; (b) the South Aral Sea.

independence of the five Mid-Asian countries, there were 80 reservoirs with each exceeding 10 million $m^3$ of water loading capacity, which held a total of 645 billion $m^3$ of water load. These reservoirs included the colossal Toktogul, Kayrakkum and Chardara in the Syr Darya River watershed, and the Nurek Hydroplant in the Amu Darya River watershed. In particular, build-up of the many large canals and water diversion projects in the Aral Sea watershed had expanded the irrigation area of the five countries to 8.1 million ha (Gafurov et al., 2010). In the 1960s, the Aral Sea shrank significantly, and our results showed the lake elevation and area in the South Aral Sea continued to decrease during 2001–2015 (Fig. 3). Before the 1960s, the Aral Sea was a continuum, then was separated into two parts as Kazakhstan and Uzbekistan over-consumed the lake water to meet the demands of agriculture and industry in the basin. These anthropogenic activities and long-lasting droughts caused many ecological and environmental concerns such as lake shrinkage, land salinization, fishery crisis, and soil and vegetation deterioration.

After 1991, the Aral Sea countries decided to have a fund for ecology and conservation of the region. In particular, the Kazakhstan government initiated specific policies to conserve the North Aral Sea and began harnessing the Syr Darya River. To maintain the water level of the North Aral Sea, a dam was built in the sector, leading to a rising water table, salinity reduction, and rejuvenation of fishery. However, this also led to reduced water supply to the South Aral Sea. Fortunately, runoffs of the Syr Darya River were sufficient to maintain the water level of the North Aral Sea. However, due to anthropogenic activities with manipulated discharge and feeding, watercourses and exits of the lakes changed the nature of the sea. This may account for why the lake area and water level were relatively stable in the North Aral Sea (Figs. 4 and 5). At present, the North and South Aral Seas are occasionally connected either by groundwater dynamics or manipulative reservoir discharge.

A water crisis still existed owing to the financial deficit of Uzbekistan, leading to the desiccation of the artificial channels that connects the North and South Aral Seas. As a result, the lake area, water elevation, and lake storage of the South Aral Sea decreased during 2001–2015 (Figs. 4, 5 and 10). Cretaux et al. (2013) found that many river courses had been used for irrigation in Kazakhstan and Uzbekistan, and the lake elevation of the Aral Sea fell from about 53 m in 1989 to 30 m in 2014. A transboundary water resource management strategy for the Aral Sea region had been initiated by the Interstate Commission for Water Coordination in Central Asia (ICWC), but little has changed for the region after many years have passed. In addition, the national water resource management agencies had been merged with the agricultural department, such that the ICWC was presented with the role of implementing ecological conservation and water resource management. All these factors may add to put the situations of the Aral Sea more complex to explain.

### 4.2 Lake dynamics and SWT

The intensive agricultural activities occurring in the Aral Sea region since the 1950s have resulted in the over-consumption of the lake water, posing serious challenges to maintaining the lake storage at a stable level. In this study, we found that the lake area and ele-

vation of the South Aral Sea showed a persistent decrease throughout 2001 to 2015, and lake storage variations presented slight fluctuations in the North Aral Sea but higher variations in the South Aral Sea, consistent with Peneva et al. (2004).

Water storage of the lakes could be modulated by weather conditions and runoff scenarios. Micklin (2010) found that the water levels of the Aral Sea had dropped about 13 m, and the area shrank by 40% during 1960–1987. Peneva et al. (2004) reported that the sea volume decreased from 270 to 130 $km^3$, and the surface water area decreased from 35 000 to 22 000 $km^2$ during 1993–2000. Yoshihiro et al. (2007) also documented that the sea level in the Aral Sea fell about 4.5 m during 1993–2001, about 60 cm down per year. In short, these studies all depicted a similar course of sea level fall in the Aral Sea with respect to the lake volume or area. Desiccation of the Aral Sea has been recognized as one acute ecological challenge that may alter the water balance of the region.

Likewise, the daytime temperature and nighttime temperature showed a consistent tendency in the Aral Sea, especially in 2009, 2011, and 2013 (Fig. 7). A lake with a deeper depth can provide a higher heat capacity; thus, the lake area, elevation, and storage capacity are often correlated with the average lake depth (Gorham, 1964). Our results revealed that the lake storage variations had weak linear correlations with the daytime SWT in the South Aral Sea, and no robust relationships for nighttime SWT in the North Aral Sea, implying there may be complicated factors determining the associations ($R^2 = 0.33$, $P < 0.01$). Furthermore, for the MODIS LST products, daytime temperature variations were divided into three groups (> 1.1°C; > 0.8°C; > 0.4°C) in the South Aral Sea (Table 1). The daytime temperature variations of the South Aral Sea > 1.1°C (average LST: 1.38°C) showed moderate correlations with lake storage variations ($R^2$ from 0.53 to 0.33). Our results were also in line with Wang et al. (2018), despite of weak relationships. Regarding this subject, Yoshihiro et al. (2007) suggested that both regional climate change and irrigation regimes contributed to lake dynamics of the Aral Sea. Furthermore, according to the 2015 report by the United States Geographical Union Congress, lake surface temperatures from gauge measurements indicated a rising trend at a rate of 0.34℃ per decade during 1985–2009. Likewise, we found that the daytime temperatures showed an increase in the South Aral Sea in the past 15 yr, with a larger diurnal temperature difference. Also, land-use types of the arid Aral Sea region were mainly saline-alkaline, which might be prone to increase the near-ground air temperatures. Accordingly, higher diurnal temperature differences might result in smaller areas or shallower depths in the Aral Sea. Furthermore, the increased daytime SWT in the South Aral Sea may be a fair predictor of the decreased lake storage capacity, reflecting the co-variation in lake areas and elevation despite the increased contribution from anthropogenic activities (see Section 4.1). With the possibility of a warmer and drier future at the locality, the increased SWT in relation to complicated environmental factors may also account for the shrinking of the South Aral Sea.

### 4.3 Effectiveness of MODIS LST and ICESat/GLAS products application

Lake surface water temperature is essential for indicating lake stability and regional climate features. Using measurements from ground meteorological stations, previous studies had verified that the MODIS LST products were proper for long-term remote sensing analysis of temperature (Sima et al., 2013). Ke et al. (2014) found that the MODIS LST products for water bodies were better than that for the land surface in that the water bodies have a homogeneous surface, larger specific heat capacity, and fine spatiotemporal variability. Our results indicated that positive correlations existed between gauged temperatures and the MODIS LST ($R^2 = 0.64$; $P < 0.01$), consistent with Wan et al. (2002). This indicated that there existed some errors for remote

**Table 1** Regression equations of lake storage variations ($x$) and MODIS LST variations ($y$) during 2001 to 2015 ($P < 0.01$)

| Variations of Daytime LST of South Aral Sea (℃) | Averaged daytime LST (℃) | Regression equation | $R^2$ |
|---|---|---|---|
| > 1.1 | 1.38 | $y$=4e–05$x$+1.05 ($N$=5) | 0.53 |
| > 0.8 | 0.93 | $y$=4e–05$x$+0.92 ($N$=10) | 0.35 |
| > 0.4 | 0.61 | $y$=5e–05$x$+0.74 ($N$=14) | 0.33 |

sensing applications because of the spatial scaling difference and diverse physical properties between meteorological stations and MODIS footprints. Wan et al. (2002) reported that the major sources of uncertainties in the LST validation resided in the spatial variations in the surface temperature and emissivity within a MODIS pixel (1000 m). In particular, it might be unlikely to accurately measure the air temperature at the MODIS pixel resolution with field instruments. Meteorological measurements might be affected by lying landscapes and measuring errors of the instruments in the study area, posing certain disparities between the meteorological measurements and the MODIS LST. On the other hand, radiation, as a critical factor dominating the balance of energy coming into and leaving from the Earth-atmosphere system, could impact the land surface temperatures. This may be related to the differences between averaged daytime and nighttime MODIS LST (Fig. 7). In the daytime MODIS LST imagery, many clear sky grids with lower surface emissivity values could be observed. In addition, datasets from other stations also showed certain disparity, partly due to the fact that MODIS LST is an eight-day composite product while the meteorological measurements are daily. Finally, the essential requirements for MODIS LST product validation included adequate temperature measurements, effective MODIS pixels, homogeneous underlying surface, precise instrumentation, and less interference. However, the MODIS LST products can merely reflect variations in the lake surface water temperature. Although Xiao et al. (2013) indicated the presence of errors between satellite and actual observations, the MODIS LST were still considered fine for investigating lake thermodynamics.

Because the ICESat/GLAS was originally designed for the polar areas, the data for canopy and biomass estimates were limited in the case area (Huang et al., 2011; Zhang et al., 2011). Particularly, for those lakes with deeper lakeshores, the ICESat/GLAS provided accurate elevations with the best accuracy (Zhang et al., 2011). Nevertheless, the ICESat/GLAS data for remote lakes with shallow lakeshores may have substantial errors, despite the buffering analysis that was conducted in rows for the MODIS LST. In addition, the service time of ICESat that was used to obtain lake elevations was limited in 2003–2009, and the supplements through regressions in the South and North Aral Seas during the omitted years may result in uncertainties in estimating lake elevation and storage, compared to the actual elevation.

### 4.4 Research uncertainties

Long-term lake dynamics can help unveil the climate and ecological changes of a region. In this study, variations in lake area, elevation and storage were examined, as well as the SWT. However, there were still many uncertainties associated with the remote sensing of lake dynamics and SWT. First, in this study, we identified the stable shared boundary of the lake in each year by extraction from the MODIS temperature imagery. However, this process often neglected the influence of seasonal lake area changes between seasons (rainy or dry season) that implied the alterations of SWT. Second, although the SWT extracted from MOD11A2 had a consistent temporal resolution (8-day gridded products), with MOD09A1 used for extracting the area of the Aral Sea, the relatively lower spatial resolutions between MOD11A2 (1000 m) and MOD09A1 (500 m) were different, which may have affected the final results. In addition, the mixed pixels at the land/water interfaces for the MODIS 8-day composite images could result in potential uncertainties in the observations of the long-term dynamics. Cai et al. (2016) reported that for Poyang Lake and Dongting Lake, the differences between the MODIS- and Landsat-delineated inundation areas (high resolution: 30 m) were 10.31% and 11.53%, respectively. These uncertainties should be lower for bodies of water with larger areas or storage on account of the relatively slight influences of mixed pixels. Next, obtaining the lakebed topography of the Aral Sea is difficult by remote sensing, which makes error-free estimates of the water storage virtually impossible (Cai et al., 2016). As a compromise, area and level-based power relationships, and MODIS-delineated inundation areas were proposed to estimate the lake storage. The Aral Sea has certain unique properties, including specific lake bed morphology, ice coverage, frozen length, and watershed land cover; each may influence the air temperature and SWT of the lake. Apart from the above, this study merely considered the influence of lake dynamics on SWT in an arid region; however, lake-ice duration, water salinity, groundwater, lakebed morphology and water color or phytoplankton existence, as well as watershed anthropogenic activities may also affect the lake SWT. There-

fore, fusion of multi-source remote sensing data may be needed to improve the spatiotemporal recognition of the mission in future studies.

## 5 Conclusions

Lake dynamics have been recognized as important information for quantifying climate variations and guiding environmental management at localities. Using MODIS LST (daytime and nighttime) products, MODIS reflectance, and ICESat observations, we examined the lake surface water temperature, area, elevation, and water storage of the Aral Sea during 2001–2015. Our results showed that there existed slight deviations between MODIS LST and field-measured air temperatures in the Aral Sea region, and the MODIS LST could be employed for tackling the lake thermodynamics.

Dynamics in the area and elevation of the Aral Sea have been observed. The area and elevation of the North Aral Sea peaked in 2006 and exhibited relative stability afterward, indicating the likely effects of regional water resource regulation and conservation efforts in the basin. By contrast, lake area, elevation, and storage of the South Aral Sea shrank due to intensive irrigation, droughts, and financial deficit.

Furthermore, lake surface daytime and nighttime temperatures in the North Aral Sea exhibited a decrease, while the daytime temperatures in the South Aral Sea revealed an increase, with a higher diurnal temperature difference. The correlations between SWT and lake dynamics (area and elevation) were all weak ($P > 0.05$). A weak correlation was also found between the daytime temperature variations and lake storage variations ($R^2 = 0.33$, $P < 0.05$) in the South Aral Sea. This demonstrated that climate change and anthropogenic impacts may overlap to yield complicated consequences in the Aral Sea.

## References


Bai J, Chen X, Li J et al., 2011. Changes in the area of inland lakes in arid regions of central Asia during the past 30 years. *Environmental Monitoring and Assessment*, 178(1–4): 247–256. doi: 10.1007/s10661-010-1686-y

Boomer I, Wünnemann B, Mackay A W et al., 2009. Advances in understanding the late Holocene history of the Aral Sea region. *Quaternary International*, 194(1–2): 79–90. doi: 10.1016/j.quaint.2008.03.007

Cai X, Feng L, Hou X et al., 2016. Remote sensing of the water storage dynamics of large lakes and reservoirs in the Yangtze River Basin from 2000 to 2014. *Scientific Reports*, 6: 36405. doi: 10.1038/srep36405

Chen J L, Wilson C R, Tapley B D et al., 2017. Long-term and seasonal Caspian Sea level change from satellite gravity and altimeter measurements. *Journal of Geophysical Research*: *Solid Earth*, 122(3): 2274–2290. doi: 10.1002/2016JB013595

Cretaux J F, Letolle R, Bergé-Nguyen M, 2013. History of Aral Sea level variability and current scientific debates. *Global and Planetary Change*, 110: 99–113. doi: 10.1016/j.gloplacha.2013.05.006

Crosman E T, Horel J D, 2009. MODIS-derived surface temperature of the Great Salt Lake. *Remote Sensing of Environment*, 113(1): 73–81. doi: 10.1016/j.rse.2008.08.013

Dessler A E, Palm S P, Spinhirne J D, 2006. Tropical cloud-top height distributions revealed by the ice, cloud, and land elevation satellite (ICESat)/Geoscience laser altimeter system (GLAS). *Journal of Geophysical Research*: *Atmospheres*, 111(D12). doi: 10.1029/2005JD006705

Gafurov A, 2010. *Water Balance Modeling Using Remote Sensing Information: Focus on Central Asia*. Stuttgart: University of Stuttgart.

Gong P, 2012. Remote sensing of environmental changes over China: a review. *Chinese Science Bulletin*, 57: 2793–2801. doi: 10.1007/s11434-012-5268-y

Gorham E, 1964. Morphometric control of annual heat budgets in temperate lakes. *Limnology and Oceanography*, 9(4): 529–533. doi: 10.4319/lo.1964.9.4.0525

Hu Liangjun, Yang Haijun, Yang Qinke et al., 2010. A GIS-based modeling approach for fast assessment of soil erosion by water at regional scale, Loess Plateau. *Chinese Geographical Science*, 20(5): 423–433. doi: 10.1007/s11769-010-0416-2

Huang X, Xie H, Liang T et al., 2011. Estimating vertical error of SRTM and map-based DEMs using ICESat altimetry data in the eastern Tibetan Plateau. *International Journal of Remote Sensing*, 32(18): 5177–5196. doi: 10.1080/01431161.2010.495092

Ke L H, Song C Q, 2014. Remotely sensed surface temperature variation of an inland saline lake over the central Qinghai–Tibet Plateau. *ISPRS Journal of Photogrammetry and Remote Sensing*, 98: 157–167. doi: 10.1016/j.isprsjprs.2014.09.007

Livingstone D M, Dokulil M T, 2001. Eighty years of spatially coherent Austrian lake surface temperatures and their relationship to regional air temperature and the North Atlantic Oscillation. *Limnology and Oceanography*, 46(5): 1220–1227. doi: 10.4319/lo.2001.46.5.1220

Luyssaert S, Jammet M, Stoy P C et al., 2014. Land management and land-cover change have impacts of similar magnitude on surface temperature. *Nature Climate Change*, 4: 389–393. doi: 10.1038/nclimate2196

McFeeters S K, 1996. The use of the Normalized Difference Water Index (NDWI) in the delineation of open water features. *International Journal of Remote Sensing*, 17(7): 1425–1432. doi: 10.1080/01431169608948714

Micklin P, 2010. The past, present, and future Aral Sea. *Lakes & Reservoirs: Research & Management*, 15(3): 193–213. doi: 10.1111/j.1440-1770.2010.00437.x

Peneva E L, Stanev E V, Stanychni S V et al., 2004. The recent evolution of the Aral Sea level and water properties: analysis of satellite, gauge and hydrometeorological data. *Journal of Marine Systems*, 47(1–4): 11–24. doi: 10.1016/j.jmarsys.2003.12.005

Riordan B, Verbyla D, McGuire A D, 2006. Shrinking ponds in subarctic Alaska based on 1950–2002 remotely sensed images. *Journal of Geophysical Research: Biogeosciences*, 111(G4). doi: 10.1029/2005JG000150

Shi K, Zhang Y, Zhu G et al., 2015. Long-term remote monitoring of total suspended matter concentration in Lake Taihu using 250 m MODIS-Aqua data. *Remote Sensing of Environment*, 164: 43–56. doi: 10.1016/j.rse.2015.02.029

Shi K, Zhang Y, Zhang Y et al., 2019. Phenology of Phytoplankton Blooms in a Trophic Lake Observed from Long-term MODIS Data. *Environmental Science & Technology*, 53: 2324–2331. doi: 10.1021/acs.est.8b06887

Sima S, Ahmadalipour A, Tajrishy M, 2013. Mapping surface temperature in a hyper-saline lake and investigating the effect of temperature distribution on the lake evaporation. *Remote Sensing of Environment*, 136: 374–385. doi: 10.1016/j.rse.2013.05.014

Song K, Wang M, Du J et al., 2016. Spatiotemporal variations of lake surface temperature across the Tibetan Plateau using MODIS LST product. *Remote Sensing*, 8(10): 854. doi: 10.3390/rs8100854

Sun F, Sun W, Chen J et al., 2012. Comparison and improvement of methods for identifying waterbodies in remotely sensed imagery. *International journal of Remote Sensing*, 33(21): 6854–6875. doi: 10.1080/01431161.2012.692829

Wan Z, Zhang Y, Zhang Q et al., 2002. Validation of the land surface temperature products retrieved from terra moderate resolution imaging spectroradiometer data. *Remote Sensing of Environment*, 83(1–2): 163–180. doi: 10.1016/S0034-4257(02)00093-7

Wang J, Song C, Reager J T et al., 2018. Recent global decline in endorheic basin water storages. *Nature geoscience*, 11(12): 926. doi: 10.1038/NGEO2999

Wang X, Gong P, Zhao Y et al., 2013. Water-level changes in China's large lakes determined from ICESat/GLAS data. *Remote Sensing of Environment*, 132: 131–144. doi: 10.1016/j.rse.2013.01.005

Wang X W, Cheng X, Li Z et al., 2012. Lake water footprints identification from time-series ICESat/GLAS data. *IEEE Geoscience and Remote Sensing Letters*, 9: 333–337. doi: 10.1109/LGRS.2011.2167495

Wang Z M, Song K S, Zhang B et al., 2009. Shrinkage and fragmentation of grasslands in the West Songnen Plain, China. *Agriculture, Ecosystems and Environment*, 129: 315–324. doi: 10.1016/j.agee.2008.10.009

Xiao F, Ling F, Du Y et al., 2013. Evaluation of spatial-temporal dynamics in surface water temperature of Qinghai Lake from 2001 to 2010 by using MODIS data. *Journal of Arid Land*, 5(4): 452 464. doi: 10.1007/s40333-013-0188-5

Zhang G, Xie H, Kang S et al, 2011. Monitoring lake level changes on the Tibetan Plateau using ICESat altimetry data (2003–2009). *Remote Sensing of Environment*, 115(7): 1733–1742. doi: 10.1016/j.rse.2011.03.005

Zhang S, Gao H, Naz B S, 2014. Monitoring reservoir storage in South Asia from multisatellite remote sensing. *Water Resources Research*, 50(11): 8927 8943. doi: 10.1002/2014WR015829